communications biology

Article

https://doi.org/10.1038/s42003-024-06664-x

Preventing periprosthetic osteolysis in aging populations through lymphatic activation and stem cell-associated secretory phenotype inhibition

Chen Zhao[1,5], Kewei Rong[1,5], Pengcheng Liu[2,5], Keyu Kong[1], Haikuo Li[3], Pu Zhang[1], Xuzhuo Chen[4], Qiang Fu[2] ✉ & Xiaoqing Wang[1] ✉

With increases in life expectancy, the number of patients requiring joint replacement therapy and experiencing periprosthetic osteolysis, the most common complication leading to implant failure, is growing or underestimated. In this study, we found that osteolysis progression and osteoclast differentiation in the surface of the skull bone of adult mice were accompanied by significant expansion of lymphatic vessels within bones. Using recombinant VEGF-C protein to activate VEGFR3 and promote proliferation of lymphatic vessels in bone, we counteracted excessive differentiation of osteoclasts and osteolysis caused by titanium alloy particles or inflammatory cytokines LPS/TNF-α. However, this effect was not observed in aged mice because adipogenically differentiated mesenchymal stem cells (MSCs) inhibited the response of lymphatic endothelial cells to agonist proteins. The addition of the JAK inhibitor ruxolitinib restored the response of lymphatic vessels to external stimuli in aged mice to protect against osteolysis progression. These findings suggest that inhibiting SASP secretion by adipogenically differentiated MSCs while activating lymphatic vessels in bone offers a new method to prevent periprosthetic osteolysis during joint replacement follow-up.

Total joint arthroplasty (TJA) is a surgical procedure in which diseased joints are replaced with artificial joint prostheses (usually made of metals, polymer polyethylene, or ceramics) to relieve joint pain and restore joint function. Advancements in TJA technology have resulted in significant improvements in pain, mobility, and quality of life have been achieved[1]. In 2010, 719,000 total knee arthroplasties (TKAs) and 332,000 total hip arthroplasties (THAs) were performed in the United States. By 2030, these numbers are projected to increase significantly, with TKAs expected to grow by 673% to 3.48 million procedures and THAs by 174–572,000 procedures[2–4].

Periprosthetic osteolysis is a leading cause of failure in TKA and Hip Arthroplasty THA[5–7]. Periprosthetic osteolysis is a major contributor to implant loosening after TJA and often requires revision surgery. The occurrence rate of this complication can be as high as 10% within the first 20 years postoperatively[8]. In this process, tiny particles released by the implanted prosthesis promote differentiation of the surrounding osteoclasts, leading to dissolution of the adjacent bone tissue. Dissolved bone tissue loses its ability to provide adequate support for the prosthesis, creating a vicious cycle. However, therapeutic targets aimed at reducing osteoclastic bone-resorbing activity or inflammation development, including the use of bisphosphonates, a monoclonal antibody targeting the receptor activator of NFκB ligand (RANKL), and antibodies against pro-inflammatory cytokines (TNF-α and IL-1β), have proven ineffective in preventing pathological bone loss or extending the lifespan of implants[9,10]. Moreover, interventions conducted after bone resorption cannot prevent implant displacement and changes in biomechanical stress lines. Therefore, researchers should initiate preventive interventions in the early postoperative period, considering the structural characteristics of the bone's internal ecosystem.

[1]Department of Orthopedics, Shanghai Key Laboratory of Orthopedics Implant, the Ninth People's Hospital, Shanghai Jiao Tong University School of Medicine, Shanghai, China. [2]Department of Orthopedics, Shanghai General Hospital, Shanghai Jiao Tong University School of Medicine, Shanghai, China. [3]Division of Biology & Biomedical Sciences, Washington University in St. Louis School of Medicine, St. Louis, USA. [4]Department of Oral Surgery, Shanghai Key Laboratory of Stomatology & Shanghai Research Institute of Stomatology, National Clinical Research Center for Oral Diseases, Shanghai Ninth People's Hospital, College of Stomatology, Shanghai Jiao Tong University School of Medicine, Shanghai, China. [5]These authors contributed equally: Chen Zhao, Kewei Rong, Pengcheng Liu. ✉e-mail: fuqiangtj2021@163.com; osteoclast2006@163.com

Recently, the lymphatic vasculature within the skeletal system has attracted increasing attention. Ahn et al. initially confirmed the significant regulatory role of lymphatic vessels within the dorsal part of the skull in neurodegeneration[11]. Lincoln et al. verified the crucial regulatory role of the bone lymphatic system, which is activated by radiation or chemical damage during bone metabolism and repair[12]. These advancements suggest that the lymphatic network within bone is not merely an optional pathway, as previously envisioned, but may also function as a high-speed pathway that regulates physiological systems supporting bones. Owing to the prolonged presence of implants that are deeply embedded in a bone following joint replacement surgery, we hypothesized that the lymphatic system may exhibit a response to mechanical stimuli-induced bone resorption. Moreover, intervention in its expression may have a regulatory effect on bone metabolism imbalances under stress, similar to the regulatory role observed in response to radiation-induced damage. Furthermore, considering that the patient population undergoing joint replacement therapy is predominantly elderly, and Lincoln et al. demonstrated that aging inhibits the response of lymphatic endothelial cells (LECs) to genotoxic stress, we also aimed to elucidate whether the intervention role of bone lymphatic vessels in bone metabolism during periprosthetic osteolysis undergoes significant changes with aging.

In this study, we utilized a calvarial mouse model to validate changes in the proliferation of bone lymphatic vessels during osteolytic disease progression. We preliminarily determined that osteolysis can be prevented by activating the lymphatic system. However, we also found that this protective effect no longer functioned in aged mice. This is because the senescence-associated secretory phenotype (SASP) of bone marrow stromal cells (BMSCs) undergoing adipogenic differentiation in aged mice inhibits the response of the lymphatic system to exogenous lymphatic activation proteins. This inhibition can be reversed by suppressing the SASP in aged cells. These findings provide a solid foundation for the development of drugs that target the bone lymphatic system and prevent periprosthetic osteolysis after joint arthroplasty.

Results

Osteolysis involves heightened lymphangiogenesis

First, we investigated whether there were alterations in the distribution of lymphatic vessels within resorbed bone tissue as osteolysis advanced or following the formation of osteolytic lesions. To achieve this objective, we employed classical titanium alloy particles (TAP) to establish a calvarial mouse osteolysis model[13]. The micro-computed tomography (micro-CT) results indicated the successful establishment of the osteolysis model, with a significant increase in bone resorption observed from both the superior and inferior perspectives of the cranial bone compared to the control group (Fig. 1a, e). Tartrate-resistant acid phosphatase (TRAP) staining of cranial bone tissue sections after resorption revealed marked enhancement in osteoclast activity during osteolysis (Fig. 1b, f). The increased infiltration of inflammatory cells at the injury site corresponds with the active differentiation of osteoclasts and bone resorption (Fig. 1c, g). Lymphatic vessel endothelial hyaluronan receptor 1 (LYVE1) and prospero-related homeobox 1 (PROX1) are pivotal molecular markers associated with lymphatic vessel biology[12,14]. LYVE1 is a type I integral membrane glycoprotein that serves as a specific LEC marker. It plays a crucial role in mediating the interaction between LECs and hyaluronan, a key component of the extracellular matrix. PROX1 is a transcription factor and master regulator of lymphatic development and differentiation. It plays a central role in determining the fate of LECs and is essential for lymphatic vessel formation during embryogenesis. Together, LYVE1 and PROX1 serve as critical molecular markers that aid in the identification and characterization of lymphatic vessels and contribute significantly to our understanding of the molecular mechanisms underlying lymphatic vessel development, homeostasis, and function[11,15]. Mice in the TAP-treated group exhibited evident lymphatic vessel expansion in the cranial bone, characterized by a pronounced increase in the distribution of LYVE1-positive and PROX1-positive lymphatic vessels within the resorbed cranial bone tissue compared with the control group (Fig. 1d, h, i). In summary, metal particle-induced osteolysis was accompanied by changes in the proliferation and expression of markers of intraosseous lymphatic vessels, suggesting a possible regulatory role for lymphatic vessels in the bone regeneration process.

Inhibition of intraosseous lymphatic proliferation alone is sufficient to increase osteoclast activity and bone destruction

The objective of our study was to ascertain whether the proliferation of intraosseous lymphatic vessels is beneficial or detrimental to osteolysis. We aimed to determine whether bone resorption was promoted or inhibited in response to proliferation. To achieve this, we used a specific inhibitor of lymphatic proliferation, SAR131675. While VEGFR3 is an established regulator of lymphangiogenesis, SAR131675 is a selective inhibitor. Previous studies have confirmed its significant inhibitory effect on lymphatic vessel proliferation within bone[12,16]. We found that administration of SAR131675 alone on the surfaces of cranial bone for two weeks without concomitant TAP treatment was sufficient to induce a discernible degree of osteolysis (Fig. 2a, e). Moreover, TRAP staining indicated a significant enhancement of osteoclast differentiation activity in the cranial bone induced by SAR131675-mediated osteolysis (Fig. 2b, f). This further indicated that sole administration of SAR131675 was sufficient to induce osteoclast activity and, consequently, increase the area of cranial bone resorption. The results of H&E staining also revealed a significant concurrent increase in the infiltration of inflammatory cells (Fig. 2c, g). Simultaneously, the results of immunofluorescence (IF) experiments confirmed specific inhibition of lymphatic vessels, as evidenced by the suppression of lymphatic endothelial cell markers LYVE1 and PROX1 (Fig. 2d, h, i). In conclusion, these results showed that inhibition of intraosseous lymphatic vessels may promote osteolysis due to the loss of osteoclast activity suppression.

Activating intraosseous lymphatic vessels counteracts bone resorption

Because the preceding results confirmed the inhibitory effect of intraosseous lymphatic vessel suppression on bone destruction and promotion of bone resorption, we sought to determine whether preventive promotion of excessive activation of intraosseous lymphatic vessels can mitigate periprosthetic osteolysis. To achieve this, we used TAP in combination with VEGF-C recombinant protein to induce local osteolysis. Recombinant VEGF-C is a recognized essential inducer of lymphangiogenesis[17,18]. Micro-CT revealed evidence of cranial bone resorption on both the superior and inferior surfaces of bones as early as the 7th day after TAP treatment (Fig. 3a, e). However, concurrent administration of recombinant VEGF-C significantly restrained the expansion of the resorption area and initiation of bone resorption during the early stages of osteolysis (Fig. 3a, e). By the 14th day of TAP treatment, when bone resorption had fully developed and the resorption area was extensive, sustained use of VEGF-C protein exhibited notable control and improvement of osteolysis. Notably, from an inferior perspective of the cranial bone, there were no apparent perforations in the cranial base in the TAP + VEGF-C group (Fig. 3a, e). TRAP staining further demonstrated that on the 7th and 14th day post-treatment with TAP, concurrent administration of recombinant VEGF-C protein significantly inhibited osteoclast differentiation and quantity (Fig. 3b, f). This aligned with the micro-CT results. Correspondingly, there was also an improvement in the infiltration of inflammatory cells (Fig. 3c, g). Furthermore, this antagonistic effect against bone resorption was achieved by targeting intraosseous lymphatic vessels, as evidenced by the IF results. During the early stages of the bone resorption process (on the 7th day) or at a later stage (on the 14th day), significant improvement in bone resorption induced by recombinant VEGF-C protein treatment was accompanied by substantial proliferation of intraosseous lymphatic vessels. This was evidenced by the notable enrichment of LYVE1-positive cells and PROX1-positive cells (Fig. 3d, h, i).

Following this, we further validated the therapeutic effects of VEGF-C in cell experiments. Surprisingly, direct application of VEGF-C not only

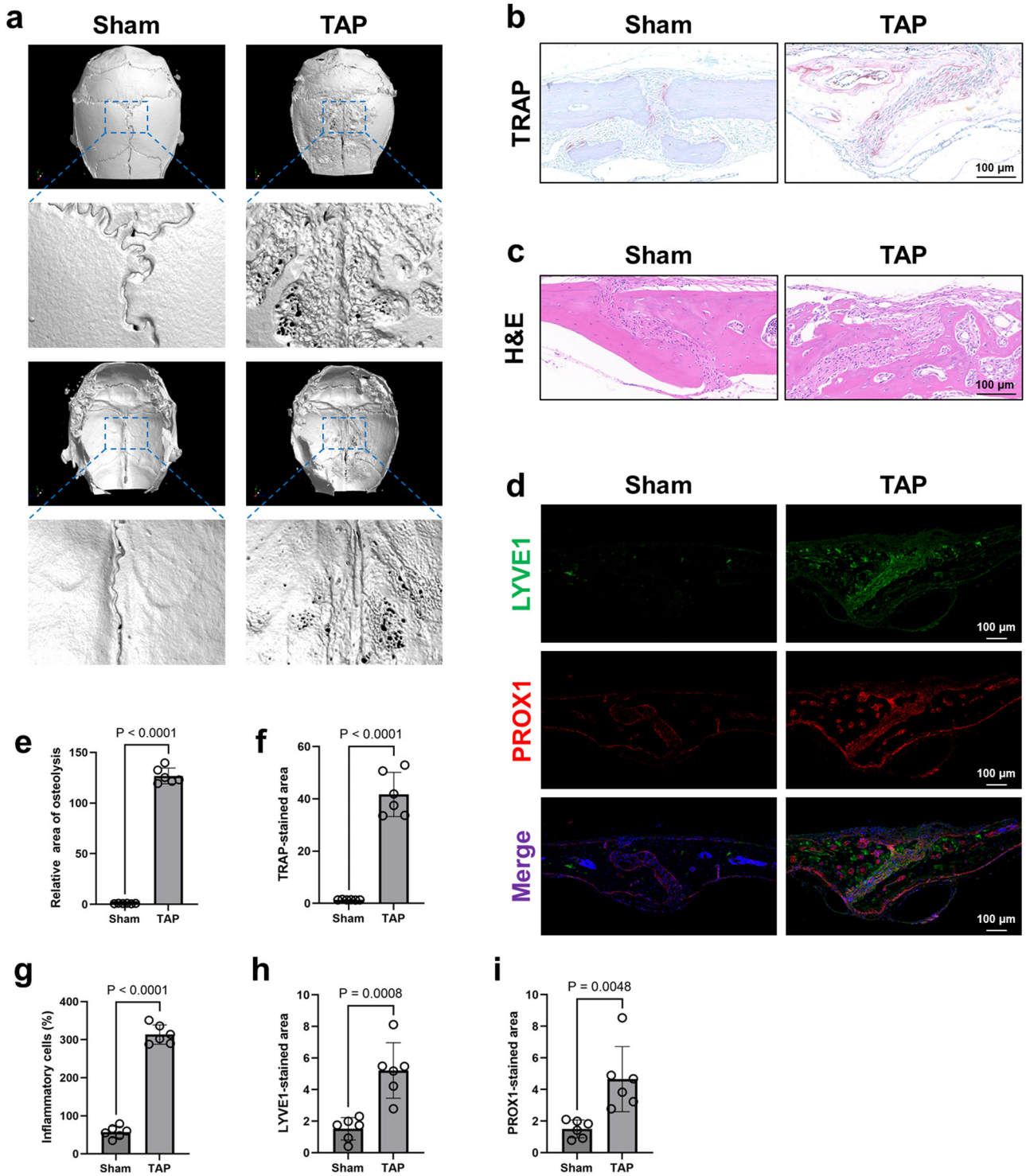

Fig. 1 | Osteolysis involves heightened lymphangiogenesis. a Micro-CT images displaying bone resorption in the cranium from both superior and inferior perspectives. **b** TRAP staining in mouse cranial bones after TAP implantation. Scale bars: 100 μm. **c** H&E staining in mouse cranial bones after TAP implantation. Scale bars: 100 μm. **d**, IF staining for DAPI with LYVE1 (green) and PROX1 (red). Scale bars, 100 μm. **e** Quantification of the lytic area in calvarial bone tissues analyzed by micro-CT ($n = 6$). **f** Quantification of TRAP-stained areas in calvarial bone sections ($n = 6$). **g**, Quantification of inflammatory infiltrating cells in calvarial bone sections ($n = 6$). **h**, **i** The corresponding quantification data for LYVE1 (green) and PROX1 (red) expressions in cranial bones on day 14 after TAP treatments ($n = 6$). Data are shown as means ± SD. P values were calculated by the two-tailed Student's t-test.

failed to inhibit osteoclast differentiation but even accelerated their further differentiation compared to the control group treated solely with RANKL (Supplementary Fig. 1a, c). However, when employing a Transwell cell coculture system to coculture upper-layer lymphatic endothelial cells with lower-layer pre-osteoclasts, solely young and vigorous lymphatic endothelial cells were able to suppress the excessive differentiation of lower-layer osteoclasts (Supplementary Fig. 1b). Moreover, by further stimulating the proliferation of upper-layer lymphatic endothelial cells using VEGF-C, this inhibition of osteoclast differentiation in the lower layer was further amplified (Supplementary Fig. 1b, d). In conclusion, this study showed that,

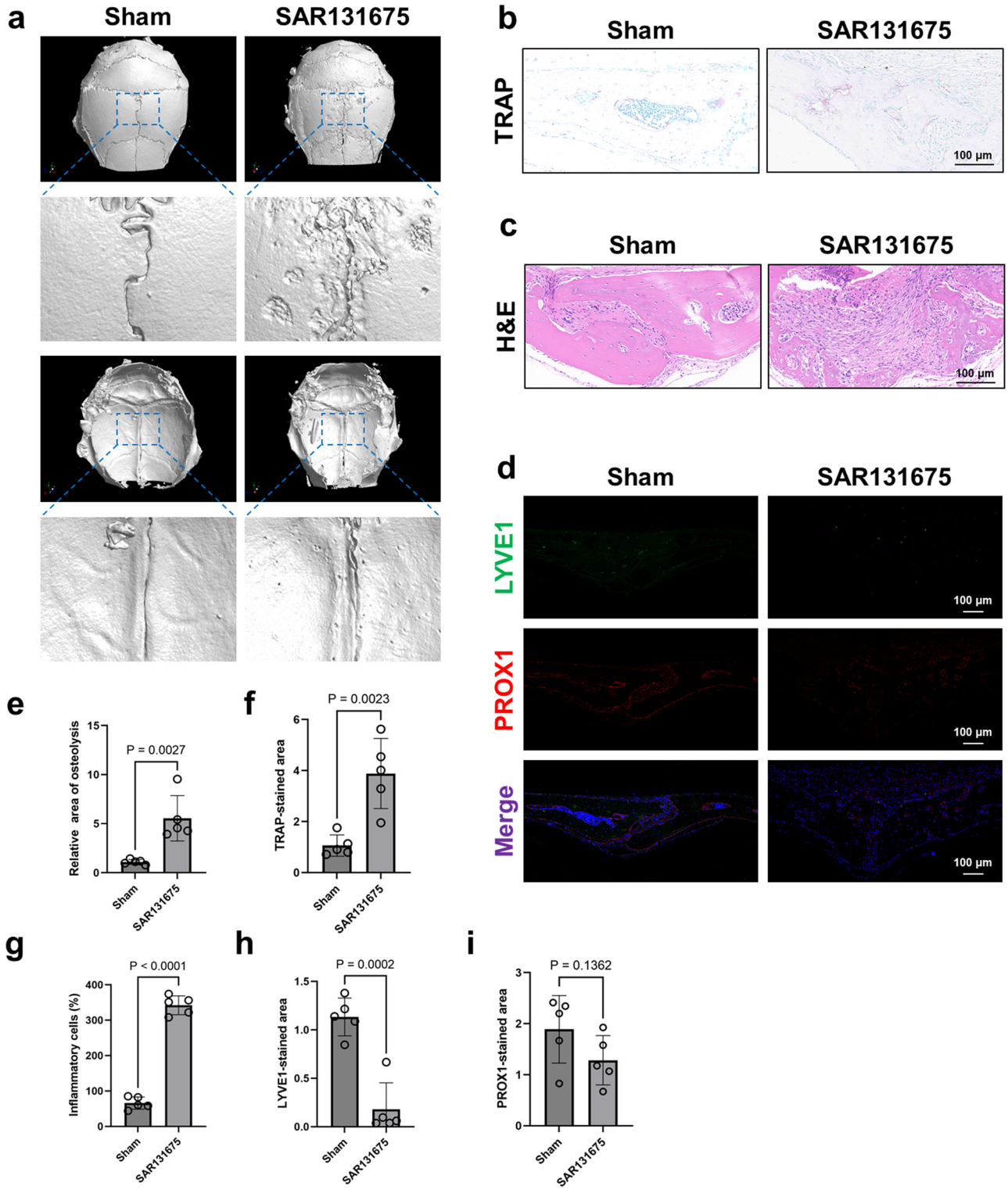

Fig. 2 | Inhibition of intraosseous lymphatic proliferation alone is sufficient to increase osteoclast activity and bone destruction. a Micro-CT images depicting cranial bone resorption from both superior and inferior perspectives after continuous treatment with SAR131675 for 14 days. **b**, TRAP staining in mouse cranial bones after SAR131675 treatment. Scale bars: 100 μm. **c** H&E staining in mouse cranial bones after SAR131675 treatment. Scale bars: 100 μm. **d** Representative IF images for LYVE1 (green) and PROX1 (red) expressions in cranial bones on day 14 after SAR131675 treatments. **e** Quantification of the lytic area in calvarial bone tissues analyzed by micro-CT ($n = 5$). **f** Quantification of TRAP-stained areas in calvarial bone sections ($n = 5$). **g** Quantification of inflammatory infiltrating cells in calvarial bone sections ($n = 5$). **h**, **i** The corresponding quantification data for LYVE1 and PROX1 expressions in cranial bones on day 14 after SAR131675 treatments ($n = 5$). Data are shown as means ± SD. *P* values were calculated by the two-tailed Student's t-test.

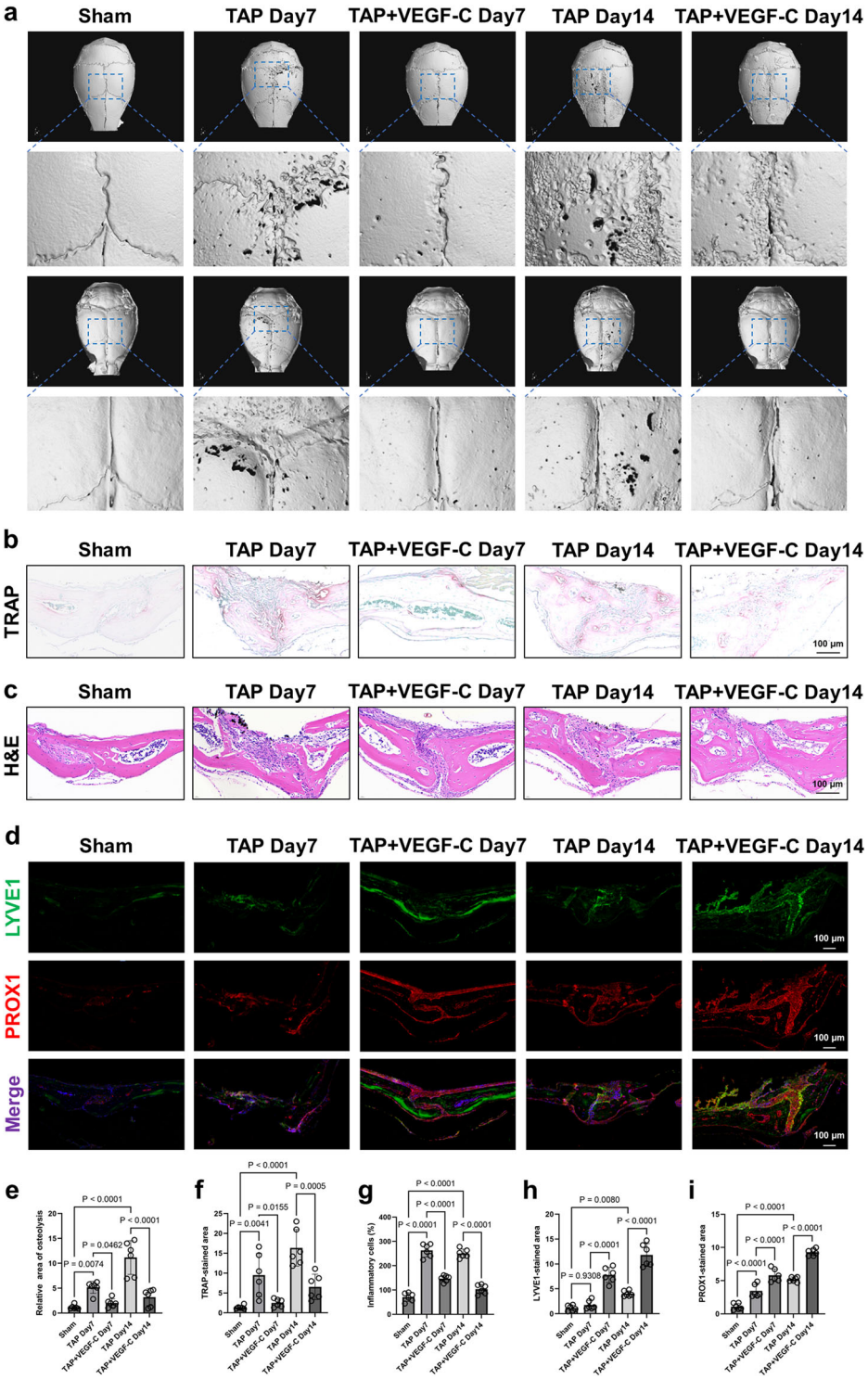

Fig. 3 | Activating intraosseous lymphatic vessels counteracts bone resorption. a Micro-CT images illustrating cranial bone resorption from both superior and inferior perspectives after continuous TAP treatment for 7 or 14 days, concomitant with subcutaneous injection of recombinant VEGF-C. **b** TRAP staining in mouse cranial bones following TAP implantation, combined with recombinant VEGF-C injection. Scale bars: 100 μm. **c** H&E staining in mouse cranial bones following TAP implantation, combined with recombinant VEGF-C injection. Scale bars: 100 μm. **d** IF staining for DAPI with LYVE1 (green) and PROX1 (red). Scale bars, 100 μm. **e** Quantification of the lytic area in calvarial bone tissues analyzed by micro-CT ($n = 6$). **f** Quantification of TRAP-stained areas in calvarial bone sections ($n = 6$). **g** Quantification of inflammatory infiltrating cells in calvarial bone sections ($n = 6$). **h**, **i** The corresponding quantitative data for LYVE1 (green) and PROX1 (red) expressions in cranial bones on day 7 or day 14 after combined TAP and recombinant VEGF-C treatments ($n = 6$). Data are shown as means ± SD. Significance was assessed through one-way ANOVA.

with concomitant administration of VEGF-C targeting and promotion of intraosseous lymphatic vessel proliferation, both early- and late-stage osteolysis induced by TAP can be significantly suppressed. This is consistent with earlier findings that inhibiting intraosseous lymphatic vessel proliferation promotes osteoclast activity.

Therapeutic effect of VEGF-C on pathological bone loss induced by LPS and TNF-α administration

To gather additional evidence of the potential therapeutic applications of lymphatic vessel proliferation in pathological bone resorption-related diseases, we treated models of lipopolysaccharide (LPS) and tumor necrosis factor-alpha (TNF-α)-induced bone loss with recombinant VEGF-C protein.

LPS is a potent inducer of bone resorption and contributes to the pathogenesis of various bone-related disorders. When administered, LPS activates immune cells and triggers the release of pro-inflammatory cytokines such as TNF-α. These inflammatory mediators stimulate osteoclast activity, leading to increased bone resorption. This LPS-induced bone loss offers a valuable experimental model for investigating the molecular and cellular mechanisms underlying pathological bone

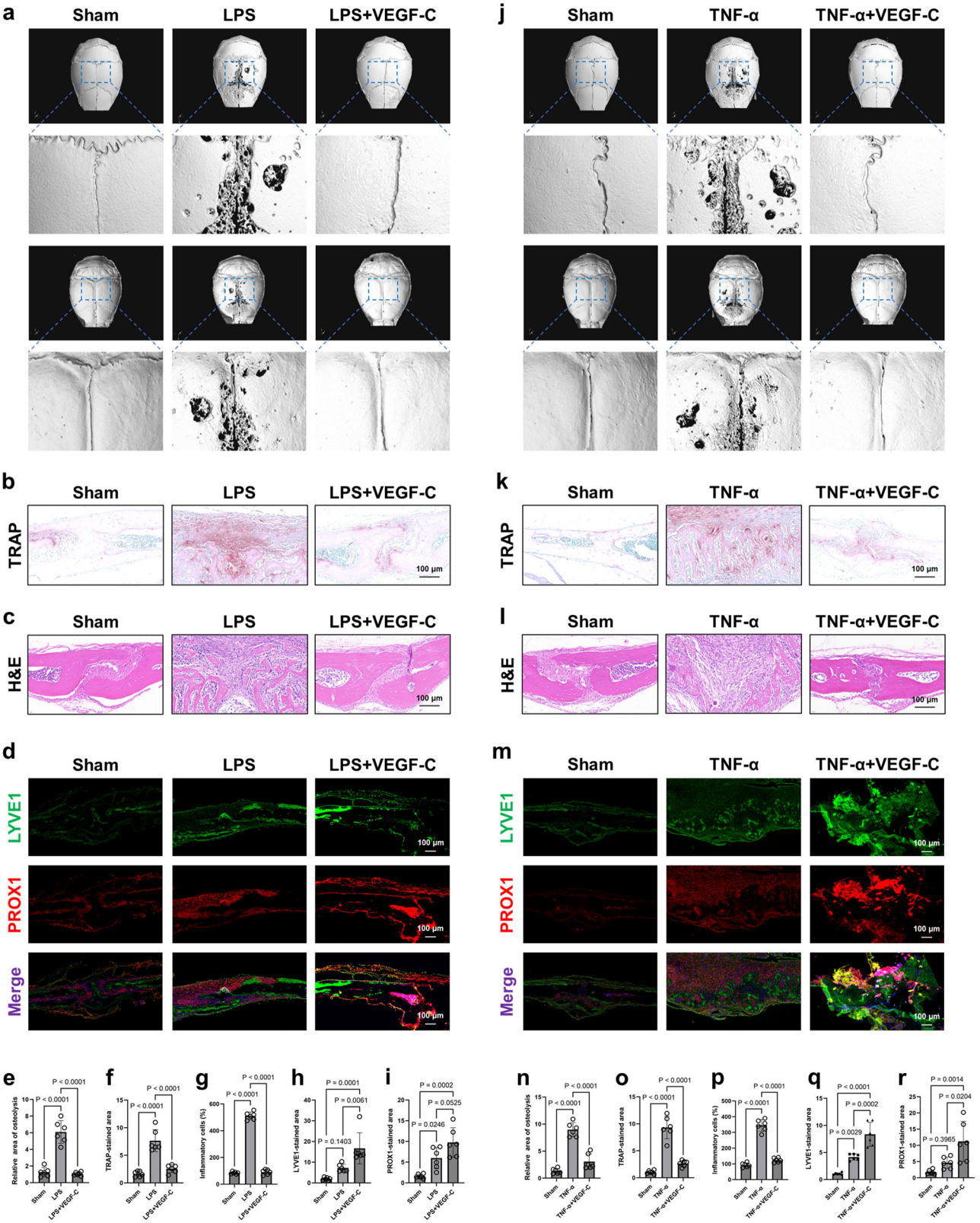

resorption[19,20]. As anticipated, local injection of LPS in mice resulted in signs of cranial bone resorption, accompanied by significant upregulation of osteoclast activity. However, these effects on induced bone resorption and osteoclast differentiation were markedly reversed upon concurrent administration of the lymphatic vessel proliferation activator VEGF-C. Notably, therapeutic improvements in LPS-induced cranial bone resorption achieved with VEGF-C treatment surpassed those observed in the model induced by TAP (Fig. 4a–c, e–g). Similarly, LPS treatment induced reactive proliferation of intraosseous lymphatic vessels concurrent with the induction of cranial bone resorption. However, concurrent treatment with VEGF-C accentuated lymphatic vessel proliferation (Fig. 4d, h, i).

Fig. 4 | Therapeutic effect of VEGF-C on pathological bone loss induced by LPS and TNF-α administration. **a** Micro-CT images depict cranial bone resorption from both superior and inferior perspectives after continuous LPS treatment for 14 days, concomitant with subcutaneous injection of recombinant VEGF-C. **b** TRAP staining in mouse cranial bones following LPS treatment, combined with recombinant VEGF-C injection. Scale bars: 100 μm. **c** H&E staining in mouse cranial bones following LPS treatment, combined with recombinant VEGF-C injection. Scale bars: 100 μm. **d** IF staining for DAPI with LYVE1 (green) and PROX1 (red). Scale bars, 100 μm. **e** Quantification of the lytic area in calvarial bone tissues analyzed by micro-CT ($n = 6$). **f** Quantification of TRAP-stained areas in calvarial bone sections ($n = 6$). **g** Quantification of inflammatory infiltrating cells in calvarial bone sections ($n = 6$). **h**, **i** The corresponding quantitative data for LYVE1 (green) and PROX1 (red) expressions in cranial bones on day 14 after combined LPS and recombinant VEGF-C treatments ($n = 6$). **j** Micro-CT images depict cranial bone resorption from both superior and inferior perspectives after continuous TNF-α treatment for 14 days, concomitant with subcutaneous injection of recombinant VEGF-C. **k** TRAP staining in mouse cranial bones following TNF-α treatment, combined with recombinant VEGF-C injection. Scale bars: 100 μm. **l** H&E staining in mouse cranial bones following TNF-α treatment, combined with recombinant VEGF-C injection. Scale bars: 100 μm. **m** IF staining for DAPI with LYVE1 (green) and PROX1 (red). Scale bars, 100 μm. **n** Quantification of the lytic area in calvarial bone tissues analyzed by micro-CT ($n = 6$). **o** Quantification of TRAP-stained areas in calvarial bone sections ($n = 6$). **p** Quantification of inflammatory infiltrating cells in calvarial bone sections ($n = 6$). **q**, **r** The corresponding quantitative data for LYVE1 (green) and PROX1 (red) expressions in cranial bones on day 14 after combined TNF-α and recombinant VEGF-C treatments ($n = 6$). Data are shown as means ± SD. Significance was assessed through one-way ANOVA.

TNF-α is recognized for its promotion of bone resorption and osteoclast differentiation. Unlike LPS, TNF-α acts as a potent pro-inflammatory cytokine that stimulates osteoclastogenesis by directly activating osteoclast precursors[21]. Our findings indicated that recombinant VEGF-C protein can effectively mitigate TNF-α-induced cranial bone surface resorption. Notably, the efficacy of VEGF-C in ameliorating bone resorption induced by this classic inflammatory cytokine was superior to its effect on TAP-induced bone resorption (Fig. 4j, n). Correspondingly, there was a marked reversal in TNF-α-induced osteoclast differentiation and inflammatory cell infiltration (Fig. 4k, l, o, p). Furthermore, the IF results indicated that this ameliorative effect was achieved through the promotion of intraosseous lymphatic vessel proliferation (Fig. 4m, q, r). In summary, this part of the experiment confirmed that, in addition to TAP, osteolysis caused by chemical inducers such as LPS and TNF-α can be rescued by VEGF-C targeting intraosseous lymphatic vessels.

Aging inhibits the ameliorative effect of VEGF-C on osteolysis

Aging has a profound effect on the skeletal system, resulting in complex array of structural and functional changes. Moreover, most patients who require clinical joint replacement and fracture internal fixation treatment are elderly. Therefore, studies on periprosthetic osteolysis should focus on the specific background of aging. We initially used aged mice to establish a TAP-induced bone resorption model. However, in contrast to the experimental outcomes obtained in young mice, bone resorption induced by TAP in aged mice was not significantly rescued by concurrent administration of VEGF-C (Fig. 5a, b). Substantial cranial bone surface resorption persisted, indicating a disparity in the experimental conclusions obtained from experiments in aged versus younger mice. At the same time, the large number of differentiated osteoclasts and the infiltration of inflammatory cells in the lytic bone tissue could not be reduced by VEGF-C application (Fig. 5c, d, f, g). This suggests that targeting the lymphatic vasculature in aging bone tissue may not adequately rescue periprosthetic osteolysis. Next, the IF results suggested that, in aging mice, the use of VEGF-C no longer significantly promoted the proliferation of lymphatic vessels in bone tissue of the treated group compared with the simple osteolysis group (Fig. 5e, h, i). In summary, these results suggest that aging diminishes the responsiveness of the skeletal system to VEGF-C-stimulated lymphatic vessel proliferation, thereby limiting the therapeutic efficacy of promoting lymphatic vessel proliferation during periprosthetic osteolysis.

Senescent and adipogenic mesenchymal stem cells suppress intraosseous lymphatic vessel proliferation

We postulated that the inability to suppress osteoclast differentiation and alleviate bone resorption through lymphatic targeting in the aging skeletal system may be attributed to significant alterations in other factors that occur with aging, thereby interfering with the responsiveness of the lymphatic system. To address this issue, we shifted our focus to aging stem cells. Aging has significant effects on stem cells within the skeletal system, including changes in cell function and properties. During aging, proliferation and differentiation capabilities of stem cells gradually diminish, and the cells tend to undergo adipogenic differentiation rather than contribute to bone formation. Aging also causes cellular dysfunction, including decreased responsiveness to external stimuli and weakened cellular immune regulatory function. These changes may have profound effects on the overall health of the skeletal system, affecting bone density, quality, and fracture risk, thereby promoting the development of osteolysis and related diseases in older adults[22,23]. Aging BMSCs are known to develop a senescence-associated secretory phenotype (SASP); SASP factors have been shown to propagate senescence in neighboring non-senescent cells through paracrine signaling or cell-cell contact, thereby affecting the homeostasis of multiple systems within bone[24–26].

Therefore, we speculated that aging SASP molecules suppressed responsiveness of the intraosseous lymphatic system to recombinant VEGF-C. Initially, we sought to elucidate whether lymphatic vessel markers within mouse bones exhibit a decline in expression levels with advancing age. Contrary to our expectations, in mice aged 24 months, there was only a modest and statistically insignificant reduction in LYVE-1-positive LECs within the bone compared to that in younger mice. Conversely, no changes in expression were observed in LECs expressing PROX1 during the aging process (Fig. 5j–l). Aging is not associated with significant changes in the distribution and expression of intraosseous lymphatic vessels. Conversely, as mice age, markers indicative of bone marrow senescence and SASP, including p53, DNA damage marker γH2AX, and perilipin$^+$ cells, were progressively upregulated. This trend was prominent in the bone marrow of 12-month-old mice and peaked in 24-month-old mice (Fig. 5m–p).

To further elucidate the impact of mesenchymal stem cell senescence and adipogenic differentiation on intraosseous lymphatic vessel proliferation, we employed an in vitro Transwell cell co-culture technique. BMSCs isolated from adult mice were seeded in the upper chamber and cultured in adipogenic differentiation induction medium. The lower chamber contained primary LECs derived from the mice (Fig. 6a). The IF results showed that the adipogenic differentiation of BMSCs in the upper layer significantly inhibited the expression of lymphatic vessel proliferation markers LYVE1 and PROX1 in the lower LECs (Fig. 6b). Finally, to ascertain whether unresponsive lymphatic vessel proliferation in aging mice can be rescued by blocking SASP molecules released by adipogenically differentiated BMSCs, we used the JAK inhibitor (JAKi) ruxolitinib, a known inhibitor of SASP in senescent cells[23]. The results of these in vitro cell experiments suggested that adipogenically differentiated BMSCs treated with JAKi lose their inhibitory effect on the proliferation of underlying lymphatic vessels (Fig. 6b). Representative micro-CT images of the skulls of aging mice indicated that treatment with JAKi alone partially counteracted bone resorption induced by TAP. Furthermore, with co-administration of JAKi and VEGF-C, the previously observed improvement in bone resorption in aging mice with prior VEGF-C treatment was restored (Fig. 6c, g). Combined targeting of lymphatic vessels based on the suppression of SASP showed pronounced inhibition of bone resorption. Simultaneously, active osteoclasts and inflammatory cells infiltration were inhibited during osteolysis by JAKi alone and JAKi in combination with VEGF-C (Fig. 6d, e, h, i). Finally, IF

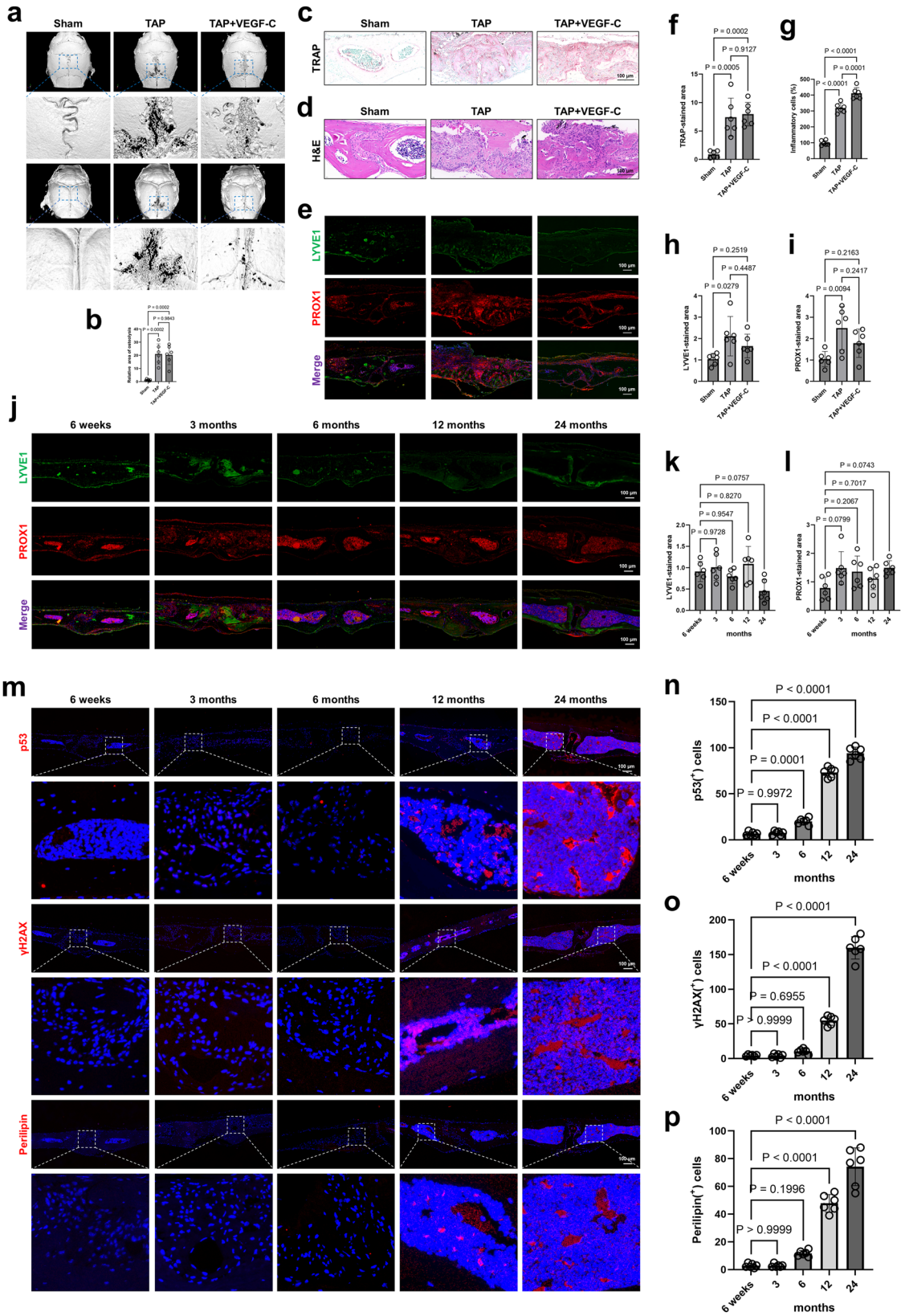

results showed effects of VEGF-C on lymphatic vessel proliferation within the bones of aging mice similar to those observed in young mice (Fig. 6f, j, k). In summary, inhibition of SASP factors secreted by senescent and adipogenically differentiated BMSCs can rescue the therapeutic efficacy of targeting lymphatic vessel proliferation during aging bone resorption.

Discussion

With aging demographics worldwide and ongoing advancements in healthcare within industrialized societies, the number of individuals requiring joint replacement surgery throughout their lifetime will inevitably surge[27]. Following implantation of internal fixation devices in the human

Fig. 5 | Aging inhibits the ameliorative effect of VEGF-C on osteolysis, accompanied by bone marrow aging and enhanced adipogenic differentiation. a Micro-CT images illustrating cranial bone resorption in aging mice from both superior and inferior perspectives after continuous TAP treatment for 14 days, concomitant with subcutaneous injection of recombinant VEGF-C. **b** Quantification of the lytic area in calvarial bone tissues analyzed by micro-CT ($n = 6$). **c** TRAP staining in aging mouse cranial bones after TAP implantation. Scale bars: 100 μm. **d** H&E staining in aging mouse cranial bones after TAP implantation. Scale bars: 100 μm. **e** IF staining for DAPI with LYVE1 (green) and PROX1 (red). Scale bars, 100 μm. **f** Quantification of TRAP-stained areas in calvarial bone sections ($n = 6$). **g** Quantification of inflammatory infiltrating cells in calvarial bone sections ($n = 6$). **h**, **i** The corresponding quantitative data for LYVE1 (green) and PROX1 (red) expressions in the cranial bones of aging mice on day 14 after combined TAP and recombinant VEGF-C treatments ($n = 6$). **j**–**l** Representative immunofluorescence images and the corresponding quantification data for LYVE1 (green) and PROX1 (red) expressions in the cranial bones of mice at different ages ($n = 6$). **m**–**p** Representative immunofluorescence images and the corresponding quantification data for p53, γH2AX and Perilipin expressions in the cranial bones of mice at different ages ($n = 6$). Data are shown as means ± SD. Significance was assessed through one-way ANOVA.

body, a noteworthy complication is periprosthetic bone resorption and consequent loosening of the implant[28–30]. If handled improperly or in an untimely manner, osteolysis around the prosthesis may seriously affect the patient's quality of life and may necessitate revision surgery. The most widely used titanium-based implants inevitably release TAP into the surrounding tissues. The concentration of TAP was found to be significantly increased at the site of peripheral implantitis, suggesting TAP as a risk factor for this disease[31–33]. Lin et al. discovered that short-chain fatty acids (SCFAs), propionic acid (C3), and butyric acid (C4) exhibited anti-inflammatory and inhibitory effects on osteoclast differentiation in wear particle-induced osteolysis following total joint arthroplasty, both in vivo and in vitro[34]. Liwei et al. showed that both genetic and pharmacological activation of Hedgehog (Hh) signaling inhibited osteoclast differentiation and activity and protected against wear particle-induced osteolysis, suggesting Hh signaling as a promising therapeutic target for the prevention and treatment of periprosthetic osteolysis and related osteolytic diseases[13]. These studies indicate the importance of small metal particles derived from prostheses in promoting and intervening in osteolysis.

Research on intraosseous lymphatic vessels has a long history. However, it was not until the early 21st century that breakthroughs in molecular biology and advanced imaging allowed the development of powerful tools to study intraosseous lymphatic vessels. Recent studies employing methods such as immunohistochemistry, microscopic imaging, and single-cell sequencing have confirmed the existence of lymphatic vessels within bones[11,12,35–37]. Further, the discovery of two lymphatic endothelial cell markers, LYVE1 and PROX1, has made it possible to quantify lymphatic vessels using simple experimental methods such as immunofluorescence and immunohistochemistry[11,12,38]. A groundbreaking study by Lincoln et al. demonstrated the promotion effect of the intraosseous lymphatic system on bone regeneration under genotoxic stress, suggesting significant therapeutic potential for various intraosseous diseases[12]. Therefore, we explored the pro-resolving function of lymphangiogenesis in periprosthetic osteolysis and assessed its therapeutic potential using experimental periprosthetic osteolysis models.

Our findings support the conclusion that lymphatic vessels exist within bone and that there is increased expression of vessel markers in a severe osteolysis model induced by metal particles. Our results also indicate that mere inhibition of intraosseous lymphatic vessels can lead to significant differentiation of osteoclasts and an osteolytic phenotype. This suggests that enhancing the proliferation of intraosseous LECs and lymphatic vessels may protect against the development of osteolysis. These conjectures were confirmed by animal experiments. Regardless of whether osteolysis was caused by titanium alloy metal particles, LPS, or the inflammatory cytokine TNF-α, application of the VEGF-C recombinant protein, which promotes proliferation of LECs[39], can inhibit the activity of intraosseous osteoclasts and osteolysis. This finding is similar to that reported by Lincoln et al.[12]. Unlike this study, however, we did not use a radiation-induced damage model but instead used a more clinically relevant osteolysis model to address common complications in orthopedic surgery.

In addition to the model of periprosthetic osteolysis induced directly by minute metal particles, the biological agents LPS and TNF-α, which can be utilized in constructing osteolysis models, were also employed in this experiment to provide a diverse range of external stimuli[20,40]. In this study, we observed that stimulation by LPS and TNF-α similarly induces excessive proliferation and activation of lymphatic vessels within the bone. Considering the reparative potential of lymphatic vessel proliferation in bone injuries, we speculate that this adaptive proliferation is also an attempt by the intraosseous ecosystem to repair damage. However, whether it is metal particles or LPS and TNF-α, they are ultimately excessive stimuli applied from outside the body at fixed frequencies, which the spontaneous repair system within the body cannot overcome. When we similarly provide continuous supplementation of VEGF-C from the external environment to counterbalance the excessive supplementation of inflammatory cytokines, the intraosseous lymphatic system, adequately supplied with "ammunition," can finally exert its full therapeutic efficacy.

Meanwhile, we also noticed that not all studies have suggested a protective role of VEGF-C in bone. Studies indicate that lymphatic vessel dilation exists in the bones of patients with Gorham-Stout disease (GSD), and mice overexpressing VEGF-C in their bones exhibit phenotypes similar to GSD[41,42]. It is noteworthy that their research did not involve direct bone destruction, unlike the radiation injury models suggesting a protective role of lymphatic vessels in bone or the direct external physical or chemical stimulation models used in this study. Therefore, in different pathological processes, the role played by activated intraosseous lymphatic vessels may vary, and excessive activation not responsive to external injury stimuli may likely have adverse effects on bone.

However, the therapeutic effect of osteolysis of targeting intraosseous lymphatic vessel proliferation was not as effective as expected in an osteolysis model established in aging mice. Therefore, we explored whether intraosseous factors limit the therapeutic effect of vessel proliferation when comparing aging and young mice. Recent studies have shown that senescent cells can promote the senescence of neighboring cells by secreting SASP factors[43,44]. The most striking feature of the aging skeletal system is the senescence of BMSCs and the resulting enhancement of adipogenic differentiation. Our results confirmed that, with an increase in the age of the mice, the expression of markers indicating BMSC aging and adipogenic differentiation gradually increased within the bone marrow cavity. Wei et al. indicated that mesenchymal stem cells (particularly MALPs) can promote differentiation and activity of osteoclasts by secreting factors such as RANKL, thereby affecting bone metabolism and remodeling[45]. With aging, adipogenic differentiation of mesenchymal stem cells intensifies, which may alter regulation of osteoclasts and further affect bone metabolism and remodeling. Leilei et al. also suggested that adipogenic differentiation of BMSCs inhibits bone formation[46]. Using a transwell co-culture technique, we were able to directly study the impact of adipogenically differentiated BMSCs on the proliferation of LECs in in vitro experiments. Our results suggest that aging and adipogenic differentiation of BMSCs inhibit LEC proliferation. We speculated that this inhibitory effect was achieved through the action of SASP molecules.

To confirm this hypothesis, we used the JAK inhibitor ruxolitinib. JAK inhibitors suppress the activity of JAK enzymes, thereby preventing cytokine transmission. In aging-related molecular phenotypes, JAK inhibitors may inhibit the JAK-STAT signaling pathway and reduce inflammatory responses, thereby inhibiting cellular aging[23,47–49]. Through cell experiments, we confirmed that inhibiting SASP factors from adipogenically differentiated BMSCs using JAKi could rescue proliferation of LECs.

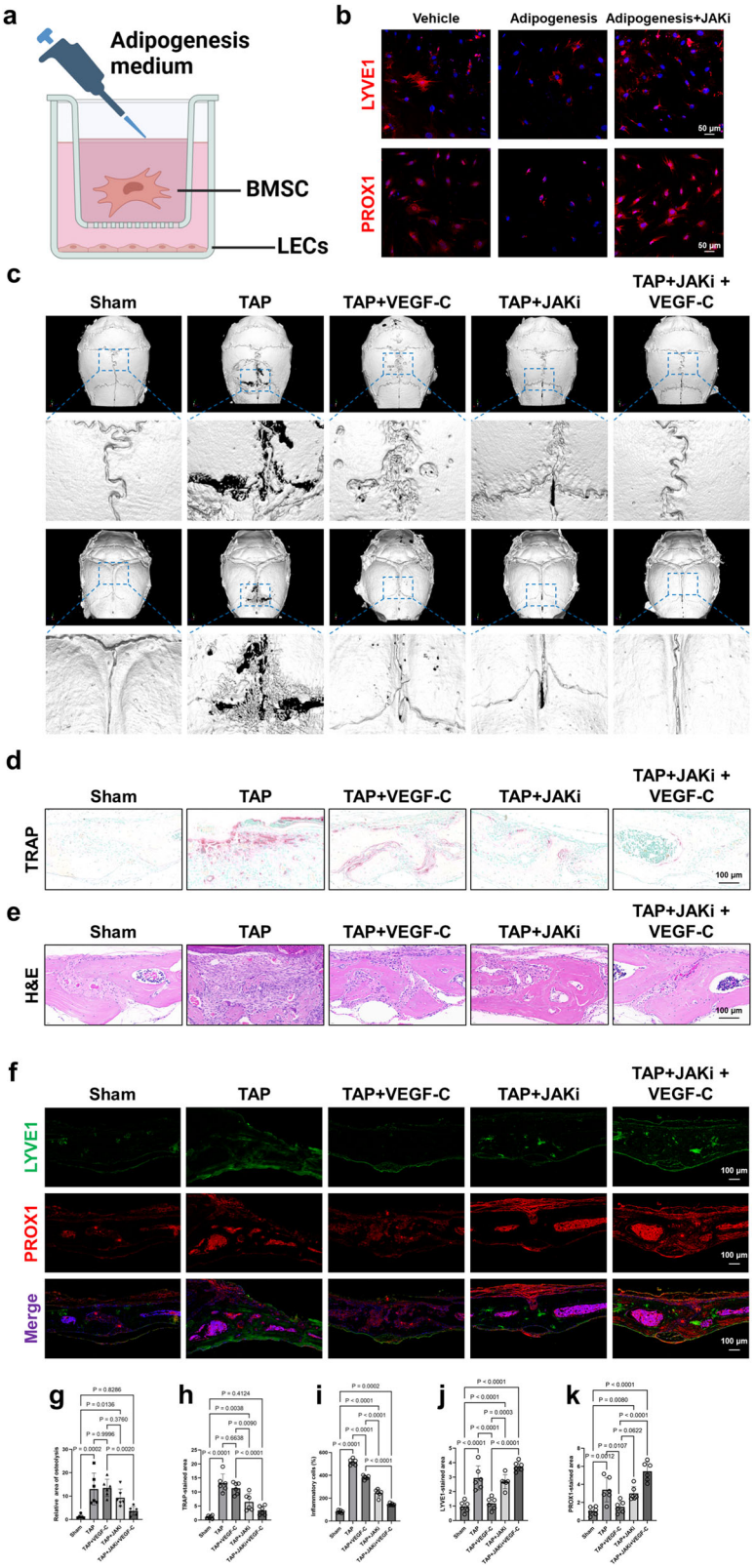

Fig. 6 | Using JAKi to inhibit SASP secretion from senescent stem cells rescues the therapeutic effect of lymphatic proliferation on osteolysis in aged mice. a Model of co-culture involving BMSCs treated with adipogenic differentiation medium and LECs. Mouse bone marrow-derived stem cells were seeded in the upper insert at a density of 5×10^4 cells/well, while the lower layer of LECs was evenly plated at a density of 1×10^5 cells/well. **b** IF images of Anti-LYVE1 antibody and Anti-PROX1 antibody demonstrate that upper-layer adipogenically differentiated BMSCs inhibit the proliferation of lower-layer LECs. However, this inhibitory effect can be reversed by using JAK inhibitor on the upper insert. Scale bar, 50 μm. **c** Micro-CT images illustrate cranial bone resorption from both superior and inferior perspectives after continuous TAP treatment for 14 days, along with subcutaneous injection of recombinant VEGF-C, oral administration of JAK inhibitor, or their combination. **d** TRAP staining was performed on mouse cranial bones following TAP treatment, combined with subcutaneous injection of recombinant VEGF-C, oral administration of JAK inhibitor, or their combination. Scale bars: 100 μm. **e** H&E staining was performed on mouse cranial bones following TAP treatment, combined with subcutaneous injection of recombinant VEGF-C, oral administration of JAK inhibitor, or their combination. Scale bars: 100 μm. **f** IF staining for DAPI with LYVE1 (green) and PROX1 (red). Scale bars, 100 μm. **g** Micro-CT images illustrating cranial bone resorption in aging mice from both superior and inferior perspectives following TAP treatment, combined with subcutaneous injection of recombinant VEGF-C, oral administration of JAK inhibitor, or their combination. **h** Quantification of TRAP-stained areas in calvarial bone sections ($n = 6$). **i** Quantification of inflammatory infiltrating cells in calvarial bone sections ($n = 6$). **j**, **k** The corresponding quantitative data for LYVE1 (green) and PROX1 (red) expressions in cranial bones on day 14 after combined TAP treatment, subcutaneous injection of recombinant VEGF-C, oral administration of JAK inhibitor, or their combination ($n = 6$). Data are shown as means ± SD. Significance was assessed through one-way ANOVA.

Animal experiments further confirmed that use of JAK inhibitors alone could partially alleviate cranial bone osteolysis induced by metal particles in aging mice. Combined use of the lymphangiogenesis activator protein VEGF-C resulted in a therapeutic effect similar to that observed in young mice, suggesting a reversal of the inhibitory effect of aging intraosseous adipogenically differentiated on BMSCs on lymphangiogenesis. Given that the patient population receiving joint replacement treatment in clinical practice is mostly elderly, this discovery provides a basis for the future development of drugs targeting intraosseous lymphatic vessels to prevent bone resorption.

This study highlighted a novel strategy for innovative therapeutic approaches to prevent implant failure. We found that promoting excessive

proliferation of intraosseous lymphatic vessels is a promising strategy to prevent periprosthetic osteolysis after joint replacement surgery. Moreover, this targeted therapeutic effect in aging individuals will require inhibition of SASP factors released from aging BMSCs.

Methods

Study approval

Animal experiments were performed in accordance with a protocol (SH9H-2023-A904-1) approved by the Institute of Animal Care and Use Committee of the Ninth People's Hospital, Shanghai Jiao Tong University School of Medicine. All mice were housed under specific-pathogen free (SPF) conditions and maintained in a controlled environment with a temperature of 21–22 °C, humidity between 40% and 50%, and a consistent 12-h light/dark cycle throughout the experiments.

Preparation of TAP

The metallic particles utilized in this research were titanium powder particles sourced from Alfa Aesar (#000681, Heysham, UK), with a purity exceeding 93% and a diameter less than 20 μm[13,50,51]. To remove endotoxins, the particles were baked at 180 °C for 6 h and then washed twice in 70% ethanol for 24 h at 25 °C[51]. Sterile particles were suspended in phosphate-buffered saline (PBS) and stored at 4 °C until further use.

Calvarial mouse model

We have complied with all relevant ethical regulations for animal use. C57BL/6 mice were used for all analyses. The mice used in this study were all male. Unless otherwise stated, the mice used in this study were mature adult mice aged 6–12 weeks. For aging studies, the mice were at least 12 months old. In experiments involving implants or drug stimulation, mice were randomly assigned to treatment groups, with littermates serving as sham controls.

For mice subjected to TAP-induced bone resorption, C57BL/6 mice were anesthetized using isoflurane inhalation according to standard protocols. Following confirmation of anesthesia, the skin over the skull was shaved, disinfected with alcohol, and incised along the midline using a sharp surgical blade. Subsequently, 30 mg of TAP (30 μL) was evenly applied to the bilateral parietal bone surface, followed by closure of the surgical incision and additional disinfection. In all sham surgery groups, mice underwent the same surgical procedure as described above, except pure PBS (30 μL) was used instead of TAP. For the cytokine-induced osteolysis model, murine LPS (Thermo Fisher) or recombinant TNF-α (PeproTech) was injected onto the surface of the calvarial bone every other day over a 14-day period at a concentration of 100 μg/kg.

For pharmacological activation of lymphatic vessels in mouse bone tissue, recombinant VEGF-C protein (SinoBiological) at a concentration of 10 μg/mL was subcutaneously injected onto the surface of the skull. An equal volume of vehicle solution was administered to the mice in the sham group as control. Both vehicle and VEGF-C recombinant proteins were administered alternate days for 7 or 14 consecutive days.

For SAR131675 treatment, C57BL/6 mice were subcutaneously injected with 100 mg/kg SAR131675 (MCE) once daily for 14 days consecutively. In the control group, sham-operated mice were injected with PBS.

For ruxolitinib (JAKi) treatment, JAKi was dissolved in 10% DMSO and administered via oral gavage at a dose of 60 mg/kg daily for 2 weeks[52].

After 7 or 14 days, the mice were euthanized under anesthesia and their harvested skull tissues were fixed by immersion in 4% paraformaldehyde. The fixed tissues were prepared for subsequent micro-CT analysis, histopathological examination, and gene and protein analyses.

Micro-CT analysis

Micro-CT was performed using a high-resolution micro-CT system (Skyscan 1275 micro-CT scanner, Bruker micro-CT, Kontich, Belgium. The scanning resolution was set at 10 μm, with X-ray energy configured at 70 kV and 200 μA, and a fixed exposure time of 300 ms. The obtained radiographic data were analyzed in ImageJ (NIH, USA) to quantify bone loss on the surfaces of calvariae[40,52].

TRAP staining

After micro-CT imaging, calvarial samples were decalcified in 10% EDTA (pH 7.4) for two weeks and embedded in paraffin. Subsequently, histological sections were prepared for TRAP staining to assess osteoclast activity. Tartrate-resistant acid phosphatase (TRAP) staining was performed using a standard protocol (Sigma-Aldrich). TRAP-positive multinucleated cells were considered osteoclasts. The stained sections were observed and imaged under a high-quality microscope (Leica DMi8). TRAP-positive osteoclasts were quantified using ImageJ software.

IF analysis

For IF staining, calvarial tissues were deparaffinised and rehydrated. Then, 5-μm sections were permeabilized with 0.2% Triton X-100, blocked with 2% BSA for 1 h, and incubated with primary antibodies (Supplementary Table 1) overnight at 4 °C. After washing, the sections were further incubated with goat anti-rabbit IgG H&L (Alexa Fluor® 555) (Abcam) or goat anti-rabbit IgG H&L (Alexa Fluor® 488) (Abcam) secondary antibodies (diluted at 1:200) for 1 h at room temperature. The stained sections were observed and imaged using a high-quality microscope (Leica DMi8). Histological scoring and quantitative IF staining analyses were performed in a double-blind manner.

Isolation and culture of LECs

Femurs and tibiae were harvested from mice, and the bones were crushed under sterile conditions. The crushed bones underwent enzymatic digestion using collagenase A (Sigma-Aldrich) at 37 °C for 45 min, and the resulting material was filtered through a 40-μm filter to obtain a single-cell suspension. CD45-positive cells were then depleted from the single-cell suspension using a BD CD45 cell depletion kit (Invitrogen, 8804-6864-74). LECs were isolated using LYVE1 antibodies raised in rabbits and a magnetic bead-based separation method. LYVE1-positive cells were separated using anti-rabbit magnetic beads (Dynabeads M-280 Sheep Anti-Rabbit, Thermo Fisher Scientific) following the manufacturer's instructions. The successfully isolated LECs were maintained in Dulbecco's modified eagle medium supplemented with 10% fetal bovine serum (FBS) and 1% penicillin–streptomycin (Gibco, Thermo Fisher Scientific, Inc.) at 37 °C with 5% CO_2.

BMSC isolation, culture, and adipogenesis differentiation

BMSC isolation, culture, and adipogenic differentiation procedures were performed according to a previously described protocol[23]. In brief, 3-month-old male C57BL/6 mice were euthanized, and their femurs and tibias were dissected. Bone marrow cells were extracted using 22-gauge syringes filled with PBS. The freshly isolated single-cell suspensions were then plated at a density of 5×10^4 cells/cm^2 in 6-well plates using BMSC growth media (α-MEM supplemented with 10% FBS and 1% penicillin–streptomycin). The cells were allowed to proliferate for 3 days before the supernatant was aspirated. The cells were rinsed three times with PBS, and the medium was refreshed three times a week. For adipogenic differentiation, mesenchymal stem cells were cultured in adipogenic media (Human Mesenchymal Stem Cell Chondrogenic Differentiation and Staining Kit, Meilunbio) for a specified number of days, with the medium changed every two days.

Tartrate-resistant acid phosphatase (TRAP) staining assay

BMDMs were plated in 96-well plates at a density of 1 × 104 cells per well and cultured with M-CSF (30 ng/mL) and RANKL (100 ng/mL), either in the presence of external monoamine. The culture medium was renewed every 2 days until osteoclast (OCs) formation was observed on day 5. Following a 20-min fixation with 4% paraformaldehyde (PFA), cells were stained with TRAP staining solution at 37 °C for 1 h. OCs were identified as TRAP-positive cells with more than three nuclei. Images were captured using an optical microscope (Olympus).

Co-cultivation of cells

We conducted cell co-culture experiments on adipogenically differentiated BMSCs and LECs according to previously described methods[53]. In this experiment, we co-cultured BMSC and LECs using 12-mm Transwell plates with a 0.4-μm pore size polyester membrane. Initially, BMSC (5×10^4 cells/well) were seeded in the upper chamber of the plates, and LECs (1×10^5 cells/well) were seeded in the lower chamber. The Transwell insert was then placed into the well, ensuring that the BMSCs in the insert were not in direct contact with the LECs in the well but that they shared the same medium, allowing for the exchange of soluble factors. The co-culture was incubated at 37 °C in a humidified atmosphere containing 5% CO_2, and the medium was changed every two days. After the desired co-culture period, the necessary analyses, including IF, were performed. The coculture of osteoclasts and LECs was carried out following the same method as described above, with the only difference being the swapping of cells between the bottom and insert plates according to the experimental design.

Statistics and reproducibility

All experiments were conducted with at least three biological replicates. The exact number of biological replicates for each experiment is detailed in the corresponding figure legends and can be found along with the raw source data in the Source Data file. Values are presented as means ± standard error (SD). Statistical analyses were performed using GraphPad Prism 8.0 (GraphPad Software). A two-tailed Student's t-test was used to compare the two groups. For comparisons involving multiple experimental groups, either one-way or two-way analysis of variance (ANOVA) as appropriate. Statistical significance was set at $p < 0.05$.

Reporting summary

Further information on research design is available in the Nature Portfolio Reporting Summary linked to this article.

Data availability

All data supporting the findings of this study are available in the article and Supplementary Information files. The source data are provided in Supplementary Data 1. Any additional requests for information can be directed to and fulfilled by the corresponding authors. The source data are provided in this report.

Received: 28 March 2024; Accepted: 31 July 2024;
Published online: 09 August 2024

References

1. Simpson, A. H. R. W. In *Musculoskeletal Infection* (ed M. Coathup) 227–282 (Springer International Publishing, 2022).
2. Kaufman, M. G., Meaike, J. D. & Izaddoost, S. A. In *Seminars in Plastic Surgery*. 066-072 (Thieme Medical Publishers).
3. Kurtz, S., Ong, K., Lau, E., Mowat, F. & Halpern, M. Projections of primary and revision hip and knee arthroplasty in the United States from 2005 to 2030. *Jbjs* **89**, 780–785 (2007).
4. Wolford, M. L., Palso, K. & Bercovitz, A. *Hospitalization for total hip replacement among inpatients aged 45 and over: United States, 2000–1010*. (US Department of Health and Human Services, Centers for Disease Control and…, 2015).
5. Harris, W. H. Wear and periprosthetic osteolysis: the problem. *Clin. Orthop. Relat. Res. (1976-2007)* **393**, 66–70 (2001).
6. Abu-Amer, Y., Darwech, I. & Clohisy, J. C. Aseptic loosening of total joint replacements: mechanisms underlying osteolysis and potential therapies. *Arthritis Res. Ther.* **9**, 1–7 (2007).
7. Sadoghi, P. et al. Revision surgery after total joint arthroplasty: a complication-based analysis using worldwide arthroplasty registers. *J. Arthroplast.* **28**, 1329–1332 (2013).
8. Xie, J. et al. PLGA nanoparticles engineering extracellular vesicles from human umbilical cord mesenchymal stem cells ameliorates polyethylene particles induced periprosthetic osteolysis. *J. Nanobiotechnol.* **21**, 398 (2023).
9. Kandahari, A. M. et al. A review of UHMWPE wear-induced osteolysis: the role for early detection of the immune response. *Bone Res.* **4**, 1–13 (2016).
10. Cobelli, N., Scharf, B., Crisi, G. M., Hardin, J. & Santambrogio, L. Mediators of the inflammatory response to joint replacement devices. *Nat. Rev. Rheumatol.* **7**, 600–608 (2011).
11. Ahn, J. H. et al. Meningeal lymphatic vessels at the skull base drain cerebrospinal fluid. *Nature* **572**, 62–66 (2019).
12. Biswas, L. et al. Lymphatic vessels in bone support regeneration after injury. *Cell* **186**, 382–397.e324 (2023).
13. Zhang, L. et al. Genetic and pharmacological activation of Hedgehog signaling inhibits osteoclastogenesis and attenuates titanium particle-induced osteolysis partly through suppressing the JNK/c-Fos-NFATc1 cascade. *Theranostics* **10**, 6638–6660 (2020).
14. Klotz, L. et al. Cardiac lymphatics are heterogeneous in origin and respond to injury. *Nature* **522**, 62–67 (2015).
15. Pawlak, J. B. et al. Lymphatic mimicry in maternal endothelial cells promotes placental spiral artery remodeling. *J. Clin. Invest* **129**, 4912–4921 (2019).
16. Alam, A. et al. SAR131675, a potent and selective VEGFR-3-TK inhibitor with antilymphangiogenic, antitumoral, and antimetastatic activities. *Mol. Cancer Ther.* **11**, 1637–1649 (2012).
17. Hominick, D. et al. VEGF-C promotes the development of lymphatics in bone and bone loss. *Elife* **7** https://doi.org/10.7554/eLife.34323 (2018).
18. Jeltsch, M. et al. Hyperplasia of lymphatic vessels in VEGF-C transgenic mice. *Science* **276**, 1423–1425 (1997).
19. Chen, X. et al. Nirogacestat suppresses RANKL-Induced osteoclast formation in vitro and attenuates LPS-Induced bone resorption in vivo. *Exp. Cell Res* **382**, 111470 (2019).
20. Chen, X. et al. Ultrasmall PtAu(2) nanoclusters activate endogenous anti-inflammatory and anti-oxidative systems to prevent inflammatory osteolysis. *Theranostics* **13**, 1010–1027 (2023).
21. Xia, Y. et al. TGFbeta reprograms TNF stimulation of macrophages towards a non-canonical pathway driving inflammatory osteoclastogenesis. *Nat. Commun.* **13**, 3920 (2022).
22. Wang, Z. X. et al. Aged bone matrix-derived extracellular vesicles as a messenger for calcification paradox. *Nat. Commun.* **13**, 1453 (2022).
23. Liu, X. et al. Oxylipin-PPARgamma-initiated adipocyte senescence propagates secondary senescence in the bone marrow. *Cell Metab.* **35**, 667–684.e666 (2023).
24. Watanabe, S., Kawamoto, S., Ohtani, N. & Hara, E. Impact of senescence-associated secretory phenotype and its potential as a therapeutic target for senescence-associated diseases. *Cancer Sci.* **108**, 563–569 (2017).
25. Coppé, J. P., Desprez, P. Y., Krtolica, A. & Campisi, J. The senescence-associated secretory phenotype: the dark side of tumor suppression. *Annu. Rev. Pathol.* **5**, 99–118 (2010).
26. Acosta, J. C. et al. A complex secretory program orchestrated by the inflammasome controls paracrine senescence. *Nat. Cell Biol.* **15**, 978–990 (2013).
27. Yu, W., Liu, C. & Bi, Z. Effect of recombinant human erythropoietin combined with iron sucrose on postoperative hemoglobin in patients undergoing artificial joint replacement. *Sci. Rep.* **13**, 18919 (2023).
28. Yin, Z. et al. The dual role of autophagy in periprosthetic osteolysis. *Front Cell Dev. Biol.* **11**, 1123753 (2023).
29. Stratton-Powell, A. A., Williams, S., Tipper, J. L., Redmond, A. C. & Brockett, C. L. Isolation and characterisation of wear debris surrounding failed total ankle replacements. *Acta Biomater.* **159**, 410–422 (2023).
30. Dixon, D. R. & London, R. M. Restorative design and associated risks for peri-implant diseases. *Periodontology* **81**, 167–178 (2019).
31. Chen, L. et al. Titanium particles in peri-implantitis: distribution, pathogenesis and prospects. *Int. J. Oral. Sci.* **15**, 49 (2023).

32. Burton, L. et al. Orthopedic wear debris mediated inflammatory osteolysis is mediated in part by NALP3 inflammasome activation. *J. Orthop. Res.* **31**, 73–80 (2013).
33. Mbalaviele, G., Novack, D. V., Schett, G. & Teitelbaum, S. L. Inflammatory osteolysis: a conspiracy against bone. *J. Clin. Invest.* **127**, 2030–2039 (2017).
34. Wu, Y. L. et al. Propionate and butyrate attenuate macrophage pyroptosis and osteoclastogenesis induced by CoCrMo alloy particles. *Mil. Med. Res.* **9**, 46 (2022).
35. Aspelund, A. et al. A dural lymphatic vascular system that drains brain interstitial fluid and macromolecules. *J. Exp. Med.* **212**, 991–999 (2015).
36. Jacob, L. et al. Anatomy and function of the vertebral column lymphatic network in mice. *Nat. Commun.* **10**, 4594 (2019).
37. Louveau, A. et al. CNS lymphatic drainage and neuroinflammation are regulated by meningeal lymphatic vasculature. *Nat. Neurosci.* **21**, 1380–1391 (2018).
38. Louveau, A. et al. Structural and functional features of central nervous system lymphatic vessels. *Nature* **523**, 337–341 (2015).
39. Li, Z. et al. Blockade of VEGFR3 signaling leads to functional impairment of dural lymphatic vessels without affecting autoimmune neuroinflammation. *Sci. Immunol.* **8**, eabq0375 (2023).
40. Alhasan, H. et al. Inhibitory role of Annexin A1 in pathological bone resorption and therapeutic implications in periprosthetic osteolysis. *Nat. Commun.* **13**, 3919 (2022).
41. Ouyang, Y. et al. Phosphate starvation signaling increases mitochondrial membrane potential through respiration-independent mechanisms. *Elife* **13** (2024).
42. Monroy, M., McCarter, A. L., Hominick, D., Cassidy, N. & Dellinger, M. T. Lymphatics in bone arise from pre-existing lymphatics. *Development* **147** https://doi.org/10.1242/dev.184291 (2020).
43. Admasu, T. D., Rae, M. & Stolzing, A. Dissecting primary and secondary senescence to enable new senotherapeutic strategies. *Ageing Res. Rev.* **70**, 101412 (2021).
44. Teo, Y. V. et al. Notch signaling mediates secondary senescence. *Cell Rep.* **27**, 997–1007.e1005 (2019).
45. Yu, W. et al. Bone marrow adipogenic lineage precursors promote osteoclastogenesis in bone remodeling and pathologic bone loss. *J. Clin. Invest.* **131** https://doi.org/10.1172/jci140214 (2021).
46. Zhong, L. et al. Single cell transcriptomics identifies a unique adipose lineage cell population that regulates bone marrow environment. *Elife* **9** (2020).
47. Philips, R. L. et al. The JAK-STAT pathway at 30: Much learned, much more to do. *Cell* **185**, 3857–3876 (2022).
48. Liu, S. et al. Tissue engineering of JAK inhibitor-loaded hierarchically biomimetic nanostructural scaffold targeting cellular senescence for aged bone defect repair and bone remolding. *Adv. Health. Mater.* **12**, e2301798 (2023).
49. Griveau, A., Wiel, C., Ziegler, D. V., Bergo, M. O. & Bernard, D. The JAK1/2 inhibitor ruxolitinib delays premature aging phenotypes. *Aging Cell* **19**, e13122 (2020).
50. Geng, D. et al. Protection against titanium particle induced osteolysis by cannabinoid receptor 2 selective antagonist. *Biomaterials* **31**, 1996–2000 (2010).
51. Shao, H. et al. Icariin protects against titanium particle-induced osteolysis and inflammatory response in a mouse calvarial model. *Biomaterials* **60**, 92–99 (2015).
52. Farr, J. N. et al. Targeting cellular senescence prevents age-related bone loss in mice. *Nat. Med* **23**, 1072–1079 (2017).
53. Zhang, L. et al. EZH2 engages TGFbeta signaling to promote breast cancer bone metastasis via integrin beta1-FAK activation. *Nat. Commun.* **13**, 2543 (2022).

Acknowledgements

This research was supported by the National Natural Science Foundation of China (82272539 to Q.F. and 81871791 to X.W.), the Cross-disciplinary Research Fund of Shanghai Ninth People's Hospital, Shanghai Jiao Tong university School of Medicine (JYJC202229 to X.W.), and the National Key Research and Development Program of China (2023YFB3813000 to X.W.).

Author contributions

C.Z. designed and performed most of the experiments, analyzed, and interpreted the data, and wrote the manuscript. K.R. assisted in designing mouse studies and provided guidance on experiments related to osteoclast differentiation and staining. P.L. assisted in fundraising efforts and supervised the entire study. K.K. contributed critical reagents. H.L. contributed to proofreading the manuscript. P.Z. and X.C. performed the experiments. Q.F. and X.W. contributed to funding, oversaw protocol logistics, and supervised the entire study.

Competing interests

The authors declare no competing interests.

Additional information

Supplementary information The online version contains supplementary material available at https://doi.org/10.1038/s42003-024-06664-x.

Correspondence and requests for materials should be addressed to Qiang Fu or Xiaoqing Wang.

Peer review information *Communications Biology* thanks the anonymous reviewers for their contribution to the peer review of this work. Primary Handling Editor: Christina Karlsson Rosenthal. A peer review file is available.